

# Repeated surging and rapid retreat of a tidewater glacier in Scotland (Younger Dryas/Greenland Stadial 1)

TOM BRADWELL<sup>1\*</sup>  and DOUGLAS I. BENN<sup>2</sup>

<sup>1</sup>Faculty of Natural Sciences, University of Stirling, Stirling, Scotland, UK

<sup>2</sup>School of Geography and Sustainable Development, University of St Andrews, St Andrews, Scotland, UK

Received 18 November 2024; Revised 5 February 2025; Accepted 17 February 2025

**ABSTRACT:** This paper presents evidence of glacier surging in the British landform record. We use new high-resolution multibeam-echosounder bathymetry data to map the submarine geomorphology of a former tidewater glacier that drained the Skye Icefield, NW Scotland, during the Younger Dryas Stadial (Greenland Stadial 1) ca. 12.9–11.7 ka. Our onshore and offshore mapping identifies a glacial landform assemblage indicative of surge-type behaviour, followed by rapid retreat and stagnation. We delimit three separate fjord-mouth advances of the Ainort Glacier — interpreted as palaeo-surges — successively decreasing in extent. During the quiescent phase of the final surge cycle, the glacier deposited a suite of cross-fjord De Geer moraines, interpreted here as annual moraines. Their pattern and spacing suggest that net annual glacier retreat rates increased significantly from around 25–75  $\text{ma}^{-1}$  to 150  $\text{ma}^{-1}$  to >300  $\text{ma}^{-1}$ , probably in the presence of seasonal sea ice. On this basis, we find that final post-surge retreat of the Ainort Glacier, from fjord mouth to marine limit (a distance of 3.5 km), was very rapid — probably taking just 20 years. Once wholly terrestrial, the glacier stagnated and did not experience further frontal oscillations. This work highlights one potential cause of asynchronous ice-mass responses in the Younger Dryas Stadial of Scotland and reinforces the importance of identifying surge-type glaciers in palaeoglaciological studies.

© 2025 The Authors *Journal of Quaternary Science* Published by John Wiley & Sons Ltd.

**KEYWORDS:** fjords; geomorphology; glacier dynamics; palaeoglaciology; Younger Dryas

## Introduction

During the Younger Dryas (YD) Stadial (=Greenland Stadial 1), Scotland hosted a large confluent ice cap complex, the West Highland Icefield (WHI), as well as numerous smaller outlying ice caps, ice fields and corrie glaciers. These various glacier systems have been reconstructed over the past ~50 years using glacio-geomorphological evidence (e.g., Gray, 1975; Sissons, 1979; Ballantyne, 1989; Benn, 1992; Bennett and Boulton, 1993; Benn and Lukas, 2006; Finlayson et al., 2011; Boston et al., 2015; Chandler et al., 2019), with the multiple mapping efforts recently collated and reviewed (Bickerdike et al., 2016, 2018). Numerical modelling experiments successfully retrodict the location, extent, volume and flow dynamics of Scotland's ice masses throughout the YD (Golledge et al., 2008, 2009). At its maximum, the YD WHI covered an area of ca. 9000  $\text{km}^2$ , similar in size to the present-day Vatnajökull ice cap in Iceland. Immediately adjacent to the WHI, but physically separated from it, the much smaller Skye or Cuillin Icefield (~155  $\text{km}^2$ ) grew in the mountains on the Isle of Skye. Several of its outlet glaciers flowed to sea level, occupying short fjords and terminating as tidewater glaciers (e.g., in Lochs Slapin, Scavaig, Sligachan and Ainort) (Fig. 1) (Ballantyne, 1989; Benn, 1991, 1997). The timing of the maximum YD glacier extent in Scotland is well constrained in only a few places. Two of these sites are on Skye, where moraines in two separate locations (Coire Fearchair and Loch Slapin) have been robustly dated using cosmogenic  $^{10}\text{Be}$  in quartz. Both sites yield uncertainty-weighted mean exposure

ages of  $12.5 \pm 0.6$  ka (Small et al., 2012; Ballantyne et al., 2016; Ballantyne and Small, 2019). Based on radiocarbon dating of glacial lake sediments, the main WHI has been shown to have reached its maximum extent later, close to the YD Stadial termination (11.7–11.5 ka BP), strongly indicating that glacier behaviour in Western Scotland was asynchronous (e.g., MacLeod et al., 2011; Lowe et al., 2019; Palmer et al., 2020). Although there is general agreement that the timing of YD glacier maxima varied spatially across Scotland, the drivers of this asynchrony remain elusive.

Glacier surges are cyclic oscillations of ice-flow velocity and mass decoupled from climate (Sharp, 1988; Benn et al., 2019). A surge is characterised by an *active* phase where mass is rapidly transferred to the glacier terminus, resulting in forward motion two or three orders of magnitude faster than in the *quiescent*, non-surging, phase. Surges are expressions of periodic dynamic internal instabilities and, therefore, glacier limits associated with surges should not be used to infer the timing of past climatic forcing events. Several studies have suggested, based on geomorphological evidence, that surges may have occurred in Scotland during the YD Stadial, in exceptional cases (Thorpe, 1991; Evans and Wilson, 2006; Bickerdike et al., 2018). Recently, Benn (2021) has argued based on multiple lines of evidence that surging glaciers were more widespread, perhaps even commonplace, in Scotland's YD Stadial ice fields. Benn (2021) proposed that landforms in numerous locations in the Scottish Highlands and islands are consistent with palaeo-surges, although more detailed studies are required to rigorously test this hypothesis.

In this article, we present strong geomorphological evidence of surging in a YD Stadial glacier in Scotland,

\*Correspondence: Tom Bradwell, as above.  
Email: tom.bradwell@stir.ac.uk

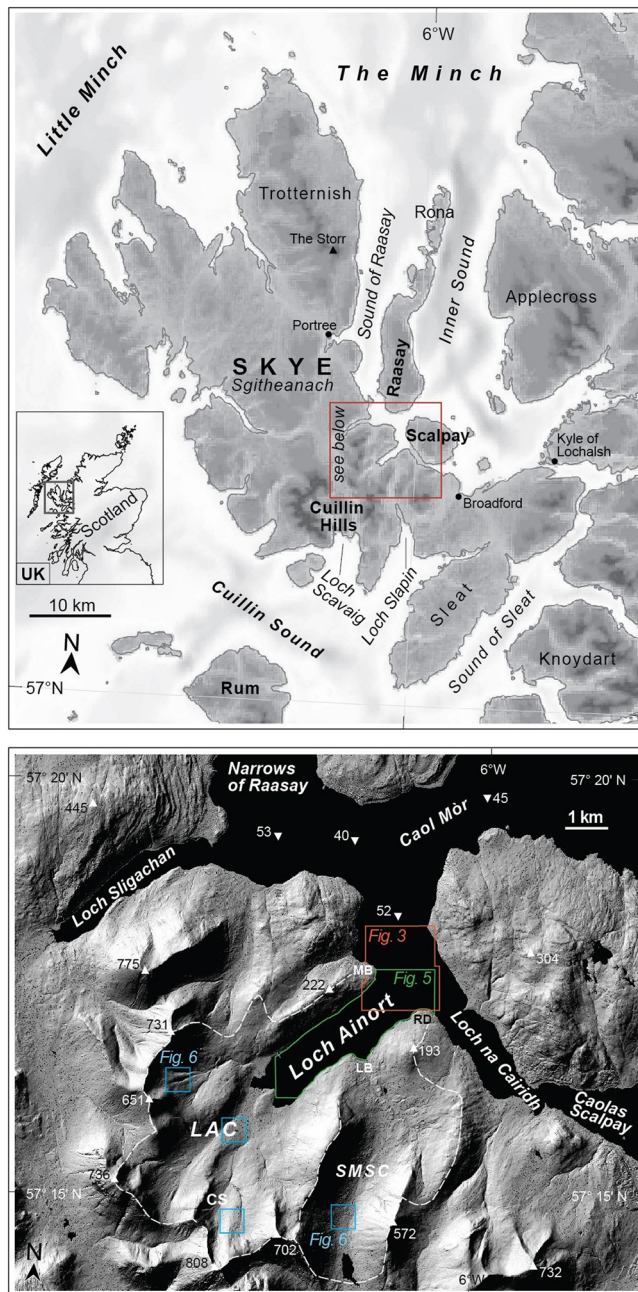


**Figure 1.** Location. Upper panel: Location of Skye in a UK/Scotland context. Topography of Skye and the surrounding seabed (greyscale ramp; darker colours, higher relief and deeper water), with key places labelled. Red box, centred on Loch Ainort, shows area of more detailed map below. Lower panel: Shaded-relief digital surface model of the Loch Ainort catchment and surrounding area. Elevation data from NEXTMap GB (Intermap Technologies); 5-m cell size; hillshade illumination from NW. CS = Coire na Seilg; LAC = Loch Ainort catchment; LB = Luib Bay; MB = Maol Ban; RD = Rubhan an h-Aird Dhuirche; SMSC = Srath Mor sub-catchment; white dashed line = catchment watershed. Selected topographic high points (in metres) and selected bathymetric water depths shown (in metres). Coloured boxes show the locations of subsequent figures (onshore and offshore). [Color figure can be viewed at [wileyonlinelibrary.com](https://onlinelibrary.wiley.com/terms-and-conditions)]

providing support for the new perspective (or new paradigm) of Benn (2021). We show that surge cycles occurred in this tidewater glacier on at least three separate occasions, leaving behind a landsystem closely resembling those deposited by modern tidewater surge-type glaciers in Svalbard. We go on to examine the nature of the quiescent phase and reconstruct post-surge ice-front retreat rates, in metres per year, based on subtle but robust geomorphological evidence.

## Methods

We use offshore and onshore geomorphological mapping and morphometric analysis to examine the well-preserved seabed landforms in Loch Ainort, NW Scotland (Fig. 1). Characterisation and analysis of the submarine geomorphology in Loch Ainort are chiefly based on new multibeam echosounder bathymetry (MBES) data collected by the UK Hydrographic Office (UKHO)/Maritime and Coastguard Agency. Terrestrial geomorphology is mapped from detailed field surveys combined with freely available high-resolution aerial photographs (Apple Maps, containing UK Ordnance Survey data; 0.25 m cell size) and radar-derived digital surface models (NEXTMap, Intermap Technologies; 5 m cell size).

The MBES data (2020 HI1569) were acquired with a Kongsberg EM3002, operating at 300 kHz, on behalf of the UKHO between March 2019 and June 2020. The raw data were processed and gridded with cell sizes at 2 m and 4 m resolution using Caris and QPS Fledermaus software; the data sets were subsequently mosaiced and merged for display and analysis in ESRI ArcGIS Pro. Submarine landform mapping was conducted manually in ArcGIS Pro from digital surface models at full resolution using various derived layers (see below). Seabed topographic profiles were extracted using geospatial analysis tools in ArcGIS Pro; morphometric data were exported to and compiled in Microsoft Excel; statistical analyses were conducted in RStudio; and cartographic presentations were finalised in Adobe Creative Suite.

Powerful semi-automated and automated GIS mapping tools are now available for landform mapping (e.g., Geomorphons (Jasiewicz and Stepinski, 2013); 3D Morphometry Toolbox (Rivers et al., 2023); and Comma Toolbox (Arosio et al., 2024)). However, we chose to map the submarine geomorphology of Loch Ainort in a GIS by delineating features via manual digitising. Although more labour-intensive, manual digitisation has the benefit of expert judgement and emphasises the key landform boundaries required for morphometric analyses. We undertook mapping using the following derivatives, all at full resolution, in addition to the processed DEM (colour ramp): 1 m elevation contours; hillshade (greyscale; multidirectional, with a vertical exaggeration value of 1.5x); slope (colour ramp); slope isolines (contours); and rugosity (colour ramp). Semitransparent DEM, contour and hillshade models were used to identify features, with slope models and slope isolines used to accurately and consistently identify crestinlines, breaks of slope and low-angle features (Fig. 2). The offshore area of interest covers 7.0 km<sup>2</sup> in total and was mapped at a range of fixed scales from 1:2500 to 1:1000 (Fig. 3). Using this optimal suite of DEM derivatives, surfaces and scales, manual digitisation allows for mapping consistency and scale-independent feature capture, permitting greater flexibility when interpreting complex multifaceted landforms that may be 'missed' or generalised using semi-automated tools. Recent work has shown that expert manual digitising performed in this way can yield superior accuracy scores compared to automated mapping tools (Arosio et al., 2024).

Morphometric data extraction, to assess landform properties, was also performed manually in this study. Our methodology broadly follows that of Rivers et al. (2023); however, we chose not to use their 3D Morphometry Toolbox as the submarine landscape of Loch Ainort contains a large number of subtle and/or fragmentary features, some of which form parts of larger landforms, as well as more complex composite landforms, mapped using expert judgement. We manually extracted data at regular intervals using readily available geospatial analysis tools in ArcGIS Pro (e.g., 3D Exploratory Analysis). For large moraines, morphological cross-profiles or transects were

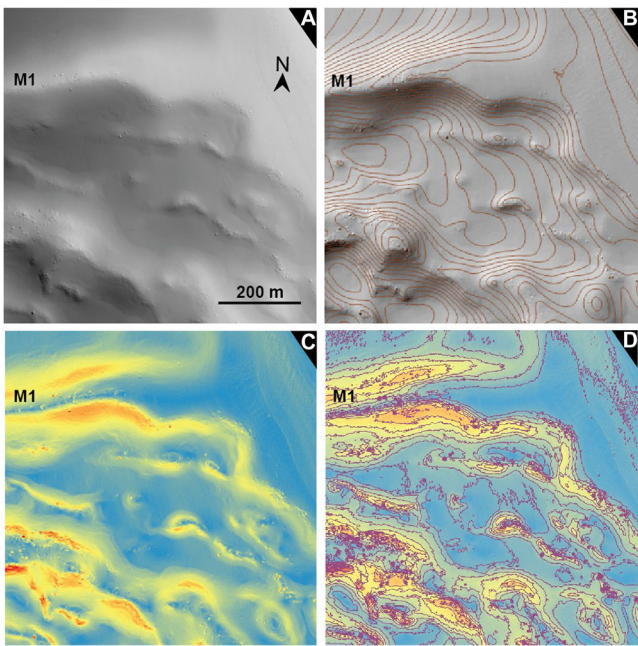


**Figure 2.** Methods. (A–D) Extracts of multibeam bathymetry data and derived digital layers used to map submarine geomorphology of Loch Ainort in this study. (A) 2-m digital elevation model with a semitransparent hillshade model overlaid; lit from NE. (B) 2-m hillshade model lit from NW with 2-m elevation contours overlaid. (C) Slope model (change in elevation); warm colours denote steeper slopes. (D) Slope model with slope isolines overlaid (lines of equal slope angle). M1 = large moraine ridge. All data are to same scale and same orientation, centred on the same point [57.2995, -6.0284]. [Color figure can be viewed at [wileyonlinelibrary.com](http://wileyonlinelibrary.com)]

digitised at 90° to feature crestlines at 100 m horizontal spacing (Fig. 4). For smaller moraines, transects were digitised at 90° to crestlines at 100 m spacings where possible; however, owing to their short length, some features only yielded one or two cross-profiles. Crest-to-crest moraine spacings were determined based on five equally spaced parallel transects trending SW–NE. These transects (T1–T5) cross-cut almost all of the smaller moraines at right angles. Where small moraines are discontinuous (in the deepest and shallowest water), straight-line joining segments were added to connect adjacent moraine fragments, perpendicular to the coastline, thereby allowing spacing calculations (Fig. 5). We recognise that other more complex moraine connections are possible.

## Submarine and terrestrial landforms: Description

Loch Ainort is a short sea loch or fjord, approximately 1 km wide and 4 km long, surrounded by steep mountains (~800 m relief) on the east coast of Skye, NW Scotland. The sea loch consists of a single basin that gradually deepens towards the fjord mouth, with the seabed reaching a maximum depth of 49 m below the present-day sea level. High-resolution bathymetry of the whole loch alongside the detailed geomorphology of the outer part and narrows between Skye and Scalpay is shown in Fig. 3. Key landform morphometrics are graphically summarised in Fig. 4, whilst the detailed geomorphology of the inner loch is shown in Fig. 5. Complete high-resolution MBES bathymetry of Loch Ainort and high-resolution aerial photograph coverage of the terrestrial part of the basin have allowed the following glacial and non-glacial landforms to be mapped, described, analysed and interpreted.

## Large arcuate moraine ridges

Three unusually large, arcuate, moraine ridge complexes (M1–M3) are mapped just beyond the fjord mouth and in the Narrows of Scalpay. The ridges form arcs extending under-water from beyond the Maol Ban headland in the north, to Scalpay in the east and the Rubha an h-Aird Dhuirche headland in the south (Fig. 3). These large moraines reach to within 9 m of the present-day sea level, with the whole nested ridge complex covering an area of 1.7 km<sup>2</sup>. Note that in the following descriptions, *proximal* refers to up-fjord (south to west)-facing slopes, whilst *distal* is down-fjord (north- to east-facing).

The outermost ridge (M1) is the largest, with a single well-developed crestline, describing a broad arc with several proximal-slope concavities or indentations in planform. This large unbroken ridge ranges from 11 to 23 m in height and from 100 to 250 m in width, and is 2.8 km long. In the east, the ridge abuts the coastline of Scalpay (below high tide) in places presenting only a proximal slope. Where best developed, M1 is generally asymmetrical in cross profile, with moderately high-angle slopes (10°–20°) and a steeper proximal slope in many places, though symmetrical sections do occur. The ridge crest is generally narrow, 10–20 m wide and undulating in height from -30 m to -8 m OD (GB Ordnance Datum). The ridge crest has high rugosity, with very large boulders common (>4 m in diameter). In the east, close to Scalpay, the M1 ridge becomes a smooth, consistent-height, flat-topped feature at 8–10 m below sea level. A large smooth (low rugosity), presumably fine-grained, lobate sediment apron mantles the flank and foot of the distal slope; in places, subtle low-angle sediment lobes are seen extending 50–200 m beyond the distal slope of the moraine ridge (Fig. 3).

Located approximately 200–300 m inshore of M1, ridge M2 is similar in arcuate planform and slightly smaller in height (6–18 m high), but with a similar width (125–250 m) to ridge M1. M2 has a broader flat-topped or double crestline along much of its length. Its cross-profile morphology is more complex than M1, suggesting a multiphase formation. At its southern end, the moraine ridge decreases in size (height and width) and appears to connect to the adjacent headland, but bathymetry data in the nearshore/intertidal zone are lacking. This large ridge is also characterised by a high-rugosity surface, with an abundance of large scattered boulders (>4 m diameter) predominantly located on ridge crests. Large blocks exceeding 8 × 8 m in size are seen in the western and central sections (Fig. 3).

Located a further 100–200 m inshore at the mouth of the sea loch, M3 is a large ridge complex similar in overall size and planform to M2 (up to 20 m high and 100–280 m wide) with two distinct crests. In the west, the M3 complex comprises twin ridges, approximately 80 m apart, with a small sediment-filled basin in between. Further to the east, the ridge complex is narrower but maintains its dual crestline. In many places, ridge asymmetry is quite marked, with steeper proximal slopes (15°–25°) and more gentle distal slopes (10°–15°). Similar to ridges M1 and M2, MBES data show that this ridge complex hosts an abundance of boulders on its surface. Connectivity with the adjacent headland to the south at the mouth of Loch Ainort is unclear. In all three complexes, ridge width and ridge height are moderately well correlated ( $r=0.61$ ;  $p<0.01$ ;  $n=3$ ), with the scatter mainly reflecting width variations along profile (Fig. 4).

Between the large arcuate moraine complexes M1 and M2 are two much smaller discontinuous arcuate ridges (2–5 m high and 30–60 m wide), separated by low-rugosity (smooth) inter-moraine sediment basins. Similar smooth, presumably

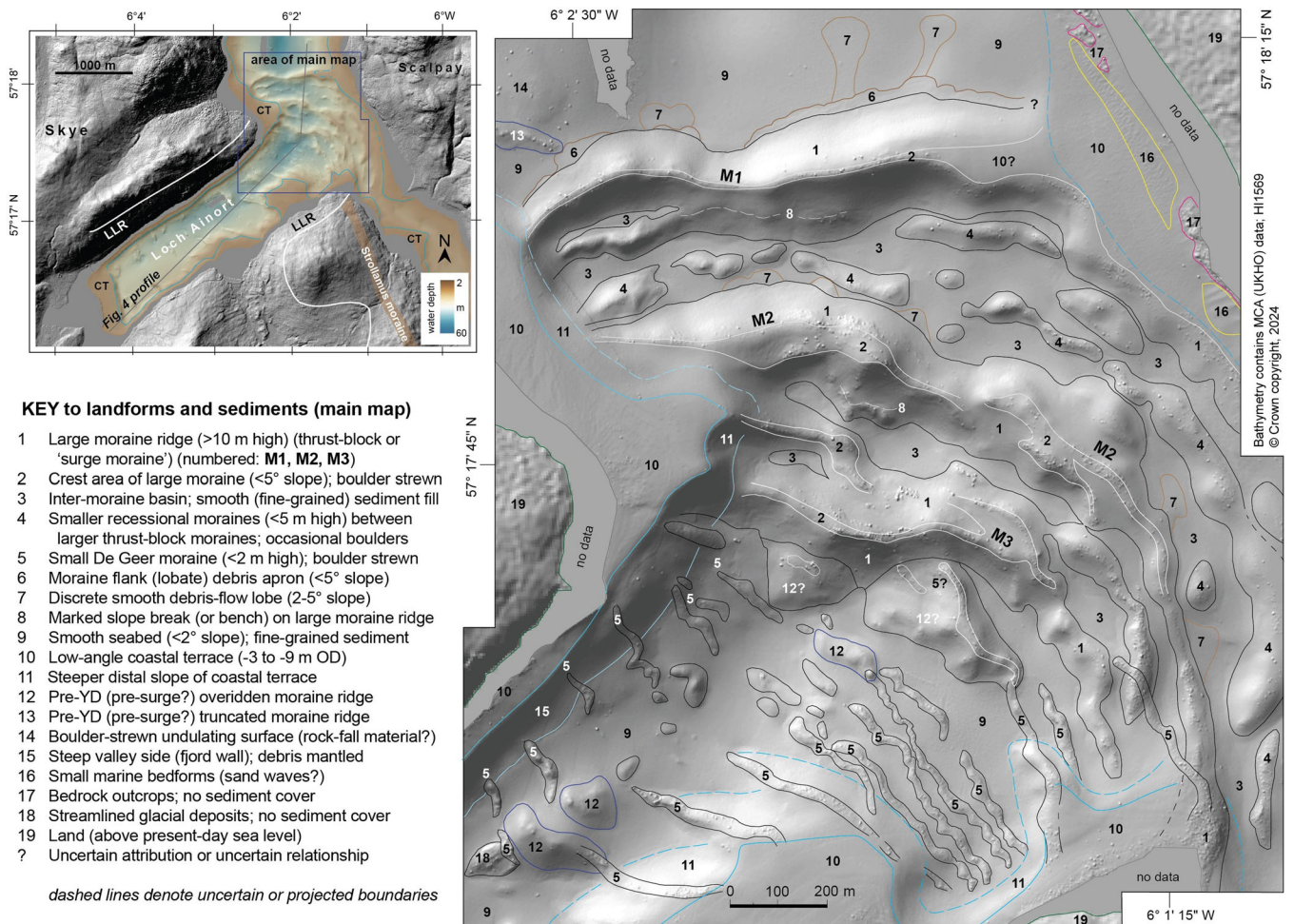


**Figure 3.** Geomorphology. Upper left panel: Combined bathymetric–topographic digital elevation model of Loch Ainort and adjacent areas (hillshade lit from NW). LLR = Loch Lomond Readvance glacier limit (from Ballantyne, 1989). CT = submerged coastal terrace; the blue line indicates the outer edge of the terrace. Location of Strollamus moraine also shown (from Benn, 1991), dated by cosmogenic-nuclide analysis to  $16.0 \pm 0.8$  ka (Small et al., 2012; Ballantyne and Small, 2019). Digital elevation model uses MBES (2-m and 4-m merged) data combined with 5-m NEXTMap GB data (both hillshade models lit from NW). The dark blue box shows the area of the main map (right). Transect (magenta line) shows the line of the bathymetric profile in Fig. 4. Main panel: Detailed geomorphological map of outer Loch Ainort overlaid on a hillshaded bathymetric digital-elevation model (lit from NW); mapped landforms are numbered and described in key. Bathymetry contains MCA (UKHO) data © Crown copyright, 2024. [Color figure can be viewed at [wileyonlinelibrary.com](http://wileyonlinelibrary.com)]

fine-grained, basin-fill sediment is also seen between ridges M2 and M3.

### Small transverse moraine ridges

The seabed of Loch Ainort is punctuated by small near-continuous to discontinuous ridges that cross the fjord perpendicular to the coastline. We map 20 (or 21) of these small transverse ridges, from the large M3 moraine to the fjord head, in water depths of 5–45 m. Typically only 0.5–2 m high, 10–30 m wide and in continuous sections up to 600 m long, these low-relief delicate ridges are well imaged on the 2-m MBES data when viewed as hillshaded surface models (Fig. 3). Most, but not all, of these minor moraines are boulder strewn. Ridges are generally linear in planform but with some curved or kinked sections. No ridge is completely continuous across the fjord, although four ridges in the outer loch cross 60%–75% of its imaged width. The gaps in the ridges generally coincide with the deepest and shallowest parts of the loch (>30 and <10 m), but we do not have data to prove whether these gaps are real (i.e., due to non-deposition or erosion) or merely apparent (i.e., due to burial by later sediments).

Our detailed mapping shows that the outermost three minor moraines overprint or merge with other (older) larger moraines, making them morphologically difficult to distinguish

and trace laterally (labelled (a)–(c) in Fig. 3). The remaining 17 (or 18) small transverse ridges are morphologically clear and form a discrete sequence from the outer loch to the fjord head. These minor moraines are numbered sequentially up-fjord (1–18) for ease of description (Fig. 5). Some are more fragmentary (e.g., 9, 11, 15), while others are more continuous (e.g., 1–5, 10, 13), but all possess the same size characteristics (<3 m high; <35 m wide), with ridge width and ridge height strongly positively correlated ( $r=0.87$ ;  $p<0.001$ ;  $n=46$ ) (Fig. 4). Ridge cross-profiles are generally asymmetric with shorter and steeper distal slopes and longer gentler proximal slopes. However, form variation exists, with some of the larger ridges (>2 m high) being more symmetrical in profile (e.g., 7, 8), whilst some of the smallest ridges have no discernible proximal slope in places, being almost step-like in cross-profile (e.g., 2, 5). Note that minor moraine 12 is very fragmentary and is mapped only with low confidence (dashed line, Fig. 5), but is included in the following morphometric analysis.

Horizontal spacing between minor moraine ridges was calculated based on five parallel longitudinal transects (T1–T5). Crest-to-crest spacing varies but shows a general increase over the 3-km distance from fjord mouth to fjord head (Fig. 5). The minor moraine suite can be broadly divided into three groups based on ridge spacings — Group 1: moraines 1–6 in the outer loch (median spacing = 65 m); Group 2:

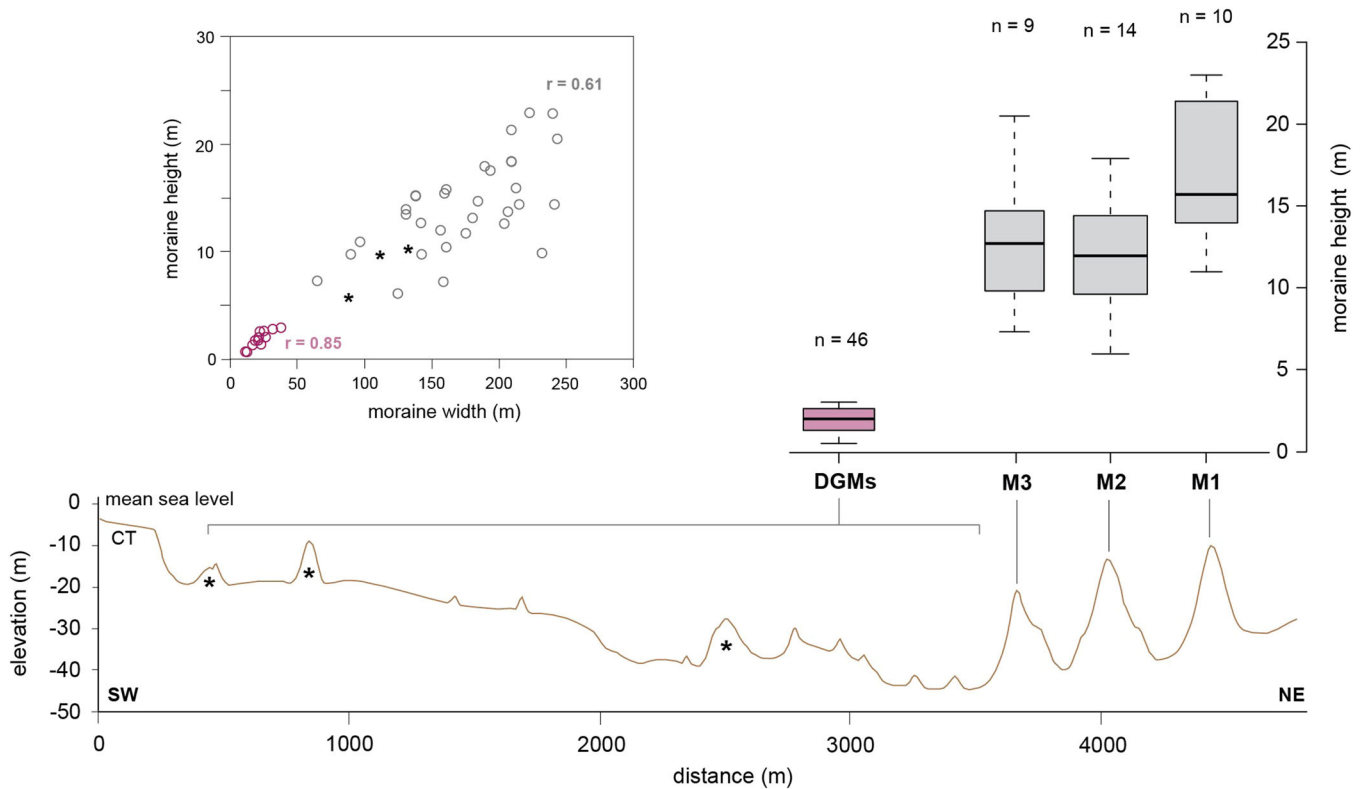


**Figure 4.** Moraine size. Lower panel: Bathymetric cross-profile along Loch Ainort (from SW to NE) showing the position and size of various seafloor moraines. DGMs = De Geer Moraines; M1, M2, M3 = large arcuate moraines. Upper right: Box-and-whisker plot of moraine height (based on multiple transects per feature). The box shows Q1–Q3 (interquartile range) data and Q2 (median); whiskers extend to 1.5IQR. Upper left: Scatter plot showing the relationship between moraine width and height. Grey circles = large moraines (M1–M3); purple circles = De Geer moraines; \*asterisks denote outsized subdued moraines, not part of the De Geer moraine population (excluded from morphometric analysis). Pearson correlation coefficients are shown. Not all De Geer moraine data points are shown for visual clarity. [Color figure can be viewed at [wileyonlinelibrary.com](https://onlinelibrary.wiley.com)]

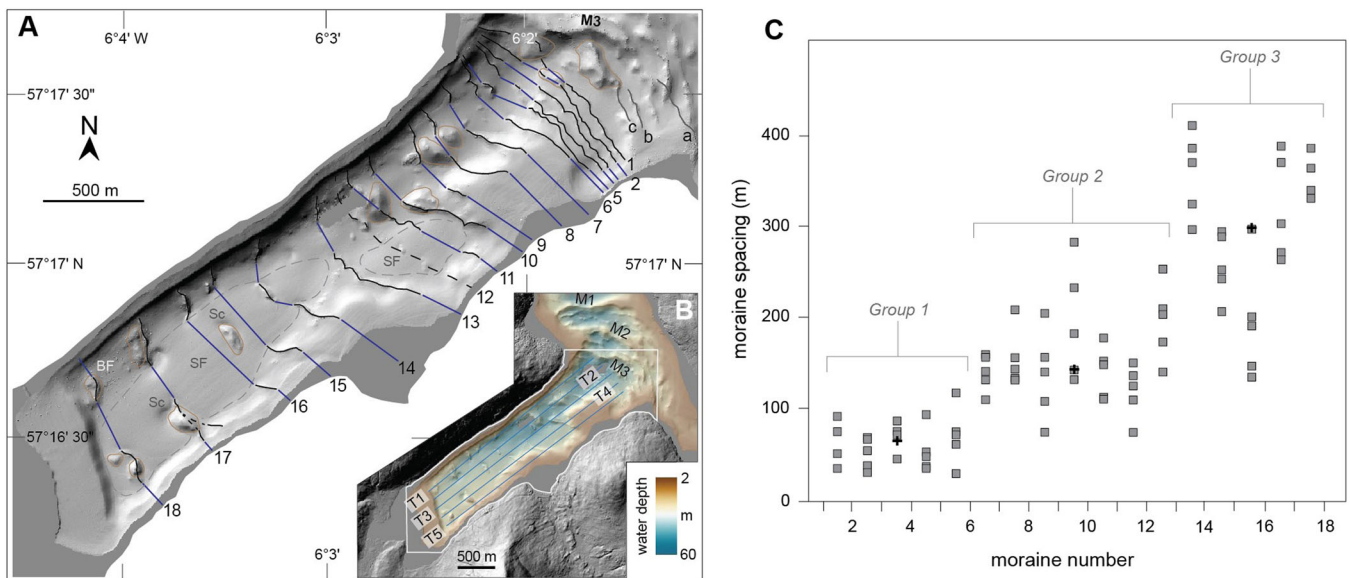


**Figure 5.** Minor moraine spacings. (A) De Geer moraines in Loch Ainort, inboard of the large arcuate moraine complexes (M1–M3). Mapped moraines (black, numbered) are connected across fjord with projected lines (blue) where moraine sections are absent. BF = boulder field; Sc = seabed scours; SF = thicker sediment fill (grey dashed line); older subdued moraine fragments also mapped (brown outline). (B) MBES bathymetry of Loch Ainort (colour ramp) showing parallel transects (T1–T5) used to measure De Geer moraine spacings. (C) Plot of crest-to-crest moraine spacings in Loch Ainort, five measurements per moraine. Note the increase in moraine spacing inshore (from moraine 1–18). The minor moraines have been classified into three groups based on these spacings. See text for more details. Bathymetry contains MCA (UKHO) data © Crown copyright, 2024. [Color figure can be viewed at [wileyonlinelibrary.com](https://onlinelibrary.wiley.com)]

moraines 7–13 in mid loch (median spacing = 143 m); and Group 3: moraines 14–18 in the inner loch (median spacing = 299 m). A non-parametric ranked-sum test (Mann–Whitney  $U$ ) finds significant differences between the three groups based on

median values (Groups 1,2:  $U = 24$ ,  $p < 0.001$ ;  $n_1 = 25$ ,  $n_2 = 35$ ; Groups 2,3:  $U = 62$ ,  $p < 0.001$ ,  $n_2 = 35$ ,  $n_3 = 25$ ). An unequal variance  $t$ -test (Welch–Satterthwaite) performed on the ranked values yields the same strong conclusion (Groups

1,2:  $t=10.13$ ;  $p<0.001$ ;  $df=58$ ; Groups 2,3:  $t=7.41$ ;  $p<0.001$ ,  $df=58$ ). Note that median values are preferred to arithmetic means for tests based on small sample sizes (five per moraine), with no assumption of normality and unequal measurement variances (per group). These data show a clear, statistically significant, increase in minor moraine spacings in Loch Ainort from the outer to the inner fjord.

### Medium to large subdued transverse moraines

Several other moderately large seabed mounds and transverse ridges occur in Loch Ainort. Most are oriented perpendicular to the fjord axis; all are fragmentary and discontinuous. These ridges are significantly larger than the suite of minor moraines, typically 5–10 m high and 60–150 m wide, with notably different shape and size properties (Figs. 4 and 5) and broad rounded crestlines. On this basis, they are excluded from the population of minor moraines. They are excluded from the population of large arcuate moraines based on their subdued discontinuous form and generally lower relief.

### Basin fill and inter-moraine sediments

Glacial and post-glacial sediment infill varies in character and thickness throughout Loch Ainort. Although we have no sub-bottom geophysical data or core material to quantify this, much can be deduced from the submarine geomorphology. The seabed between the small transverse ridges in the outer loch is generally smooth (low rugosity) but undulating, with occasional boulders indicating a (fine-grained) relatively thin sediment cover. Seabed exposures of the high-rugosity (sub-) glacial surface are seen in one or two places (e.g., between moraines 9 and 10) (Fig. 3). Further inshore, the loch floor becomes smoother (lower rugosity) and featureless between the moraines (i.e., SW of moraines 11–13). The presence of crescentic depressions or scours (2–4 m deep) flanking several seafloor mounds indicates a thicker sediment blanket here, especially in the SW part of the loch (Fig. 3). However, the presence of numerous exposed boulders on the opposite side of the loch head indicates differential subaqueous sediment deposition across the width of the fjord. Fine-grained featureless seabed is common in Scottish fjords, reflecting relatively high sedimentation rates during and following deglaciation (e.g., Stoker et al., 2009; Howe et al., 2012; Smeaton et al., 2021), with preferential deposition (along and across-fjord) typically due to sediment source proximity, reduced marine currents or action of the Coriolis force. Very little surface disturbance of the seafloor is seen in the MBES data, with no iceberg ploughmarks or grounding pits mapped. Contemporary sediment accumulation rates in Scottish fjords (over the last ~2000 years) are very low, typically  $<2\text{ mm year}^{-1}$  (Smeaton et al., 2019).

### Streamlined subglacial landforms

Onshore, in the former glacier catchment, we map low-relief elongate streamlined landforms (flutings) at several locations around Loch Ainort (Fig. 6), none of which show evidence of subsequent overprinting. The longest, subtlest flutings are seen on the southern slopes of Beinn Dearg Mhor at an elevation of 200–300 m. Individual landforms range from 50 to 250 m in length, with typical widths of 10–40 m; elongation ratios exceed 12:1 (Fig. 6). Shorter but higher relief flutings are seen on the intermediate high ground in Coire na Seilg (250–320 m asl); elongation ratios of 5–10:1 are typical here. A third setting, in Strath Mor at 10–60 m asl (Fig. 6), displays prominent lower elongation (2:1–6:1) streamlined deposits

converging to the N towards Loch Ainort. Some of these features were originally identified by Ballantyne (1989) and Benn (1991) and used to delimit the Younger Dryas extent of the glacier in this catchment. None of these landforms show evidence of burial or disturbance since glacier retreat. Natural sediment exposures are rare, but sections along the southern shore of Loch Ainort [Lat, Long: 57.2826, –6.0356] show evidence of glaciotectionism such as folded and sheared sedimentary structures in glacial till and dislocated slabs or incorporated rafts of bedrock with sediment injection features.

No clear elongate streamlined landforms are seen in the seabed MBES data; however, this may in part be due to burial by marine sediment since deglaciation.

### Boulder trains

Two unusual linear concentrations of boulders occur in the Loch Ainort catchment, originally mapped by Benn (1991) and Benn et al. (1992). The *Bruadaran erratic train* consists of a high concentration of large ( $>6\text{ m}^3$ ) Marsco granite boulders forming a narrow belt 50–80 m wide and extending for  $>3\text{ km}$  in a NE direction towards the coastline (Fig. 6). A similar erratic train 600–1000 m to the SE, composed mainly of local gabbroic (eucritic) blocks, descends obliquely across Coire na Seilg from 200–10 m asl towards the head of the loch. The boulders are typically angular in form, and appear to not have experienced subglacial transport. These two unusual boulder belt ‘moraines’ trend parallel to the streamlined subglacial bedforms described above and appear to form part of a single flow set.

### Hummocky moraine

Located between the two boulder trains is an assemblage of sand and gravel mounds, boulder-strewn hummocks, non-aligned ridges and small isolated basins (kettle holes) covering ca.  $0.3\text{ km}^2$  (Fig. 6). Unlike many other occurrences of moraines in the valleys fringing the Cuillin Hills, the moraines at the head of Loch Ainort have no discernible pattern or consistent linear elements, and are classified as chaotic hummocky moraine (Benn, 1992).

### Submerged coastal terrace

Parallel to the present-day coastline around most of Loch Ainort and in the adjacent nearshore waters is a conspicuous flat-topped terrace at water depths of 4–9 m (CT, Fig. 3). The terrace top typically slopes at  $<1^\circ$  and is fronted by a relatively uniform steep slope (typically at  $10^\circ$ – $20^\circ$ ). This submerged terrace is relatively narrow (50–100 m) but in several places, projects 300–500 m from the coast. The most conspicuous terrace projections are at the fjord head (Kinloch Ainort), at Luib Bay, NE of Luib, at Maol Ban headland, and in Loch na Cairidh (at An Dunan and Corran a Chinn Uachdaraich) (Fig. 3). In these localities, the coastal terrace resembles a sedimentary delta in shape and 3D form, extending underwater from the present-day coastline. We expect the submerged terrace to be predominantly composed of coarser-grained (glacio-)fluvial sediments deposited at the loch shore at a time of lower relative sea level (4–9 m below present). In places, the coastal terrace appears to show an erosional upper surface. It is notable that moraine M1's distinct flat-topped portion, at a water depth of 8–9 m, corresponds exactly with the elevation of the low-angle coastal terrace projecting from western Scalpay (Fig. 3).



**Figure 6.** Onshore landforms. (A–C) Elongate subglacial bedforms (flutings) onshore in Loch Ainort catchment. (A) Lower slopes of Beinn Dearg (200–350 m asl). (B) Around Lochan Sratha Mor (10–100 m asl). (C) Intermediate high ground in Coire na Seilg (250–350 m asl). (D) Ice-stagnation features at the head of Loch Ainort: (1) Marsco epigranite erratic train (within white dashed lines); (2) small circular mounds and enclosed depressions (kettle holes); and (3) unstructured morainic mounds and ridges with erratic boulders, originally mapped by Benn (1991). Imagery: 0.25-m resolution colour aerial photographs (Apple Maps, contains OS data), all at same scale. See Fig. 1 for general locations. [Color figure can be viewed at [wileyonlinelibrary.com](http://wileyonlinelibrary.com)]

## Submarine and terrestrial landforms: Interpretation

### Large arcuate moraine ridges

The large nested arcuate moraine complexes (M1, M2 M3) mark the limits of at least three advances of the former Ainort Glacier. The morphological characteristics of the arcuate moraines (i.e., unusually large size, multiple crestlines, asymmetric slopes, numerous planform indentations and debris-flow lobes or ‘mud aprons’) show strong similarities to moraines formed by surge-type tidewater glaciers in Svalbard (e.g., Ottesen and Dowdeswell, 2006; Ottesen et al., 2008; Flink et al., 2015). Particularly lobate or arcuate surge-moraine outlines are commonly seen, where the glacier exits a topographically confined fjord into more open waters (e.g., Negribreen; Ottesen et al., 2017), as is the case here. The unusual size of the nested arcuate moraines in Loch Ainort — their substantial height, width and volume — indicates a massive translocation of deformable material at the glacier margin, probably caused by high compressive stresses in the terminal zone. Their unbroken nature across the whole fjord mouth indicates a glacier firmly in contact with the bed and able to stack/thrust material along the full width of the glacier margin in a single event — something that is commonly seen in Svalbard surge-type glaciers (e.g., Ottesen and Dowdeswell, 2006). Multiple crestlines (M2 & M3) could

indicate re-occupation of the near-same position by the glacier front, or simply represent two crestlines of the same thrust-block moraine mass. Morphologically similar, equivalent-sized, subaqueous terminal moraines to M1–M3 are seen fronting Tunabreen and Borebreen in Svalbard — known surging glaciers in tidewater settings (Plassen et al., 2004; Ottesen and Dowdeswell, 2006; Flink et al., 2015; Dowdeswell et al., 2016).

The presence of distal-slope debris aprons and low-angle debris-flow lobes emanating from moraine complexes M1 and M2 is also consistent with surging. Kristensen et al. (2009) argue that these flow lobes and mud aprons form as weak saturated sediment continuously fails in front of a push/thrust moraine mass. M1 has a near-continuous, smooth, lobate apron flanking its distal slope, with several discrete low-angle lobes extending 50–200 m beyond. Only a few debris-flow lobes are seen fronting the large moraine M2, and none fronts M3; we suggest that this may be due to the lack of marine sediment availability following in the wake of the most extensive surge (M1).

### Small transverse moraine ridges

We interpret the suite of 20 (or 21) minor moraines inboard of surge moraine M3 to be *annual moraines*. This interpretation is based on strong morphological affinities with subaqueous annual moraines reported elsewhere (Fig. 4). Several studies

have shown that small (<3 m high; <30 m wide), asymmetric, closely spaced (typically <100 m), De Geer moraines in tidewater systems form with demonstrably annual frequency (e.g., Ottesen and Dowdeswell, 2006; Flink et al., 2015, 2016; Burton et al., 2016; Batchelor et al., 2019). In Svalbard (e.g., Tunabreen), their annual formation reflects low fjord-water temperatures in winter and a consequent cessation of melt-undercutting and/or calving of the ice front (Flink et al., 2015; Luckman et al., 2015). In summer, calving occurs in response to melt-undercutting, or melting of the subaqueous portion of the ice front by relatively warm fjord waters (Luckman et al., 2015; How et al., 2019). When fjord waters cool in winter and melt-undercutting ceases, the glacier terminus advances due to ongoing extension in response to longitudinal stresses at the ice front. This slow forward motion (<0.5 m day<sup>-1</sup>) is enough to produce terminus readvances in winter months. Flink et al.'s (2015) work is important, as it demonstrates that small De Geer moraines, normally associated with active retreat, can form annually at the grounding line during the quiescent phase of a surge even when ice-flow velocities are very low.

### *Subdued transverse moraines*

These are interpreted as older, over-ridden moraines, possibly marking limits of the glacier prior to more recent, more extensive (i.e., YD/Greenland Stadial 1) advances.

### *Streamlined subglacial landforms, boulder trains and hummocky moraine*

Subglacial bedforms with elongation ratios of >10:1 are normally indicative of fast ice flow (Stokes and Clark, 2002; Benn and Evans, 2014; Ely et al., 2016). Importantly, the subglacial bedforms and the boulder trains in the Loch Ainort catchment form a single, coherent flow set, with flow directions consistent with the maximum or near-maximum extent of the glacier (Benn et al., 1992). In the upper parts of the catchment, the flow set trends across slope, indicating that glacier flow directions did not adjust to the topography during retreat. In turn, this implies that the glacier was stagnant or near-stagnant during deglaciation. This conclusion is consistent with the presence of chaotic hummocky moraine on the valley floor between the boulder trains. These unstructured hummocky moraines are akin to those forming at the stagnant downwasting margins of debris-charged glaciers in Iceland and Svalbard today (e.g., Benn et al., 2003; Lovell et al., 2018; Chandler et al., 2020).

## Discussion

The onshore and offshore landscape components of the glacial landform assemblage in the Loch Ainort basin form a coherent assemblage recording fast flow, repeated advance, rapid retreat and stagnation of a tidewater palaeoglacier. The combination of rapid advance, followed by rapid retreat and stagnation, is characteristic of surging glacier landsystems (Benn et al., 2003; Benn, 2021). On the basis of morphostratigraphic and palynological evidence presented elsewhere (Ballantyne, 1989; Benn et al., 1992), we place these events in the Younger Dryas Stadial ca. 12.9–11.7 ka BP (Greenland Stadial 1). The following sections lay out the interpreted order of events and the reasoning behind our conclusions.

(i) *Surging behaviour and timing.* Based on the existence of the large multi-crested subaqueous surge–moraine complexes, we propose that the Ainort Glacier surged at

least three times, each slightly less extensive than the one before. M1 represents the earliest and most extensive surge. This outermost moraine (M1) is ~600–800 m beyond the previously established limit of YD Stadial (=Loch Lomond Readvance) glaciation in this fjord (Fig. 3) (Ballantyne, 1989; Benn, 1991), but is entirely consistent with a considerable glacier over-extension or surge in a topographically confined-to-unconfined flow setting. M2 is nested inside M1, and therefore younger than it, but corresponds almost exactly with existing YD Stadial ice-limits mapped onshore (Ballantyne, 1989; Benn, 1991, 2021) (Fig. 3). M3 sits just inside (~200 m) the previously mapped YD limit. Other timing evidence can be gleaned from geomorphological relationships near the coastline. The prominent coastal terrace and deltas, mapped in this study, fringing the fjord at –4 to –9 m OD (CT, Figs. 3 and 4) relate to a time of lower relative sea level (RSL) on Skye. Empirically derived sea-level reconstructions and GIA model output for Skye show a clear RSL lowstand –2 to –7 m OD between 12.5 and 10.0 ka (Shennan et al., 2018). This is the only time since ice-sheet deglaciation (ca. 16 ka BP; Bradwell et al., 2021) that RSLs on Skye fell to these levels (Shennan et al., 2018). The fact that the maximum elevation of the largest surge moraine (M1) coincides with the submerged terrace top adjacent to Scalpay suggests that the moraine height was controlled by sea level (Figs. 3 and 7). Moreover, the fact that no subaqueous minor moraines are seen *on top* of the coastal terrace indicates that RSLs were relatively low, probably not above –4 m OD when the minor moraines were deposited. We hereby ascribe all three surge moraines to the last glaciation of Skye (i.e., Younger Dryas Stadial) based on their proximity to previously mapped limits; morphological similarity to each other; unmodified, well-preserved, appearance; and relationship with a submerged relative sea-level feature of YD Stadial age. Initial mapping of Loch Ainort by Dix and Duck (2000) using seismic reflection and side-scan sonar profilers identified a single large terminal moraine ca. 800 m beyond the previously proposed YD glacial limit and a number of *De Geer moraines* in the outer part of the loch becoming less common in the inner part. Dix and Duck (2000) ascribed this pattern to a 'two-phase deglacial history' with a significant change in retreat style, which they linked to either a climatic control or a bathymetric 'basinal' control (Dix and Duck, 2000: p. 654). They found no evidence, morphological or stratigraphical, that the moraines pre-dated the YD Stadial. With only narrow track lines and without MBES data needed to build a complete map of the submarine landform assemblages, they were unable to capture the full geomorphic complexity in the fjord. We have developed and expanded their work here, showing that internal dynamic instabilities (surge cycle: active and quiescent phases) were probably responsible for the unusual, distinctive but well-preserved landform assemblage in Loch Ainort.

(ii) *Post-surge retreat.* Small fjord-crossing minor moraines, or De Geer moraines, in Loch Ainort chart punctuated tidewater glacier-front recession following surge advance. Assuming that our interpretation of the De Geer moraines as *annual moraines* is correct, we use the pattern and spacing of subaqueous moraines in Loch Ainort to quantify net ice-front retreat rates following the glacier's final surge

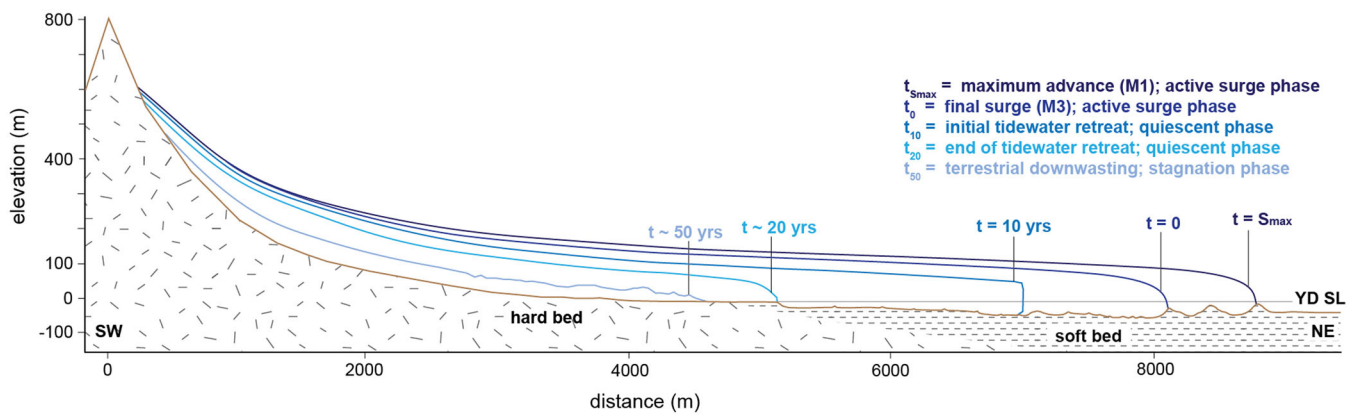


**Figure 7.** Glacier front reconstructions. 2D cross-section along the primary flow line of the former Loch Ainort glacier (from SW to NE) showing inferred Younger Dryas Stadial glacier-surface profiles at different stages during and after surge events. Both axes are to scale, but note the different scales. Horizontal (frontal) glacier retreat and timings reconstructed from annual De Geer moraine record; vertical thinning is inferred. Upper ice-surface limits are taken from previously published work (Benn et al., 1992). Hard bed (Palaeogene granite) and soft bed (Pleistocene mud, sand and gravel) extents are also shown. Soft bed thickness in Loch Ainort is uncertain. YD SL = Younger Dryas sea level. [Color figure can be viewed at [wileyonlinelibrary.com](http://wileyonlinelibrary.com)]

(Figs. 5 and 7). Annual moraine spacing (1–6) at the fjord mouth indicates grounding-line recession of ca.  $60 \text{ ma}^{-1}$  (Q1 to Q3 =  $40\text{--}75 \text{ ma}^{-1}$ ), showing limited initial recession. This rate increases significantly to ca.  $150 \text{ ma}^{-1}$  (Q1 to Q3 =  $132\text{--}183 \text{ ma}^{-1}$ ) in mid-fjord, between moraines 6 and 13. Grounding-line retreat continues to increase up-fjord (moraines 13–18), reaching rates of ca.  $300 \text{ ma}^{-1}$  (Q1 to Q3 =  $247\text{--}367 \text{ ma}^{-1}$ ) close to shore (Fig. 5). The retreat rates implied by the spacing of moraines 1–13 are similar to observed calving rates on modern tidewater glaciers in Svalbard (Flink et al., 2015; Luckman et al., 2015). Importantly, when glacier velocities are low (such as during the quiescent phase of surge cycles), calving losses are not significantly offset by advance of the ice front, and are therefore almost entirely expressed as frontal retreat. The inferred retreat rates of the Ainort Glacier in outer to mid-fjord, from moraines 1–13, are entirely consistent with those seen in modern Svalbard glaciers, if the glacier is assumed to be quiescent during recession. The rate of inferred glacier retreat in the final phase of tidewater retreat (moraines 13–18) is around double that observed in present-day Svalbard fjords. This apparent acceleration of glacier retreat could reflect climatic or oceanographic forcing (higher air or fjord water temperatures) towards the end of the YD Stadial, rather than bathymetric controls. In this part of the fjord, water depths are currently 20–30 m (Fig. 5), implying depths of perhaps only 15–25 m when the glacier was in existence. This up-fjord shallowing bathymetry is very unlikely to have exerted any influence on the rate of glacier retreat via calving. In fact, ice grounded in such shallow water may not have been subjected to high enough longitudinal stresses at the margin to drive significant forward motion. We therefore place less confidence on our inferred ice-front recession rates in the inner fjord and accept that ice may have stagnated *in situ* here without leaving a complete annual moraine record. Nevertheless, the increase in spacing from De Geer moraine 1 to 13 implies a significant acceleration of retreat up-fjord, with deglaciation of almost half the length of the fjord ( $\sim 1500 \text{ m}$ ) in just 12 years (Figs. 5 and 7).

(iii) *Final glacier retreat and stagnation.* The coherent orientation of subglacial bedforms and boulder trains and widespread ice-stagnation features show that final terrestrial retreat of the Ainort Glacier occurred by areal downwasting

rather than frontal recession (Benn, 1991, 2021). The timing and pace of this final terrestrial downwasting are currently unknown. Modern analogues, in alpine catchments, show that widespread glacier stagnation and melting normally take place over decades depending on climatic factors, but can take a century or more, especially if the ice is protected by a relatively thick debris mantle (e.g., Benn et al., 2003; Brook et al., 2013; Capt et al., 2016; Stefaniak et al., 2021). We have no way of determining the absolute pace of glacier retreat inshore of the marine limit, but we propose that it was almost certainly slower than the tidewater retreat phase based on present-day examples (Fig. 7). Interestingly, there is no evidence for partial re-growth, re-advance or re-nourishment of glaciers in the upper Loch Ainort catchment, suggesting that M3-post-surge quiescence predated the glacier's ultimate demise.

### Further support for glacier surging and wider implications

Although only about 1% of all glaciers on Earth have been classified as surge type, they are commonplace in *surge clusters* such as Iceland and Svalbard. Sevestre and Benn (2015) demonstrated that surge cluster locations are climatically controlled, and identified air temperature and precipitation limits that bound an optimal envelope for surging. Using palaeotemperatures indicated by fossil chironomid assemblages and precipitation estimates from glacier–climate relationships, Benn (2021) argued that much of Scotland, including the Isle of Skye, lay within this optimal climatic envelope during the YD Stadial. We propose that the palaeoclimatic setting, glacier hypsometry and physical environment (tidewater) of the Younger Dryas Ainort Glacier were all highly conducive to surging, for the reasons outlined below.

First, the Ainort Glacier was one of the longest glaciers in the Cuillin Icefield complex, measuring 8.8 km along its longest flow line (Fig. 7). For comparison, in Svalbard, 35% of glaciers between 8 and 16 km in length are surge type, in contrast with only 5.4% of glaciers less than 8 km in length (Benn, 2021).

Second, the Ainort Glacier had a relatively low mean surface slope of between  $3.0$  and  $3.5^\circ$  based on the reconstructed surface contours (from Ballantyne, 1989). This value is even lower ( $2.5^\circ$ ) using the new, extended, YD limits

identified here (M1; Figs. 2 and 7). Studies have shown that within surge clusters, longer, low-gradient glaciers are more likely to surge (e.g., Clarke, 1991; Jiskoot et al., 2000; Sevestre and Benn, 2015). Lower surface gradients typically produce inefficient meltwater drainage — another key factor promoting surging (e.g., Clarke, 1991; Grant et al., 2009; Sevestre and Benn, 2015; Benn et al., 2019).

Third, the trunk of the former glacier in the lower 3–4 km of the catchment flowed over a soft, easily deformable, bed comprising mainly fine-grained marine sediments (Fig. 5) (Dix and Duck, 2000). Numerous studies have identified soft beds as a necessary condition for surging, possibly due to their association with low hydraulic conductivity and inefficient basal drainage (Meier and Post, 1969; Murray et al., 2003; Benn et al., 2019; Truffer et al., 2021).

The discovery of a Younger Dryas surging glacier land-system in Loch Ainort, Skye, opens the distinct possibility of identifying other palaeo-surges in the British Isles, as noted by Benn (2021). How widespread the phenomenon was in Scotland during the Younger Dryas — and perhaps in the dwindling British and Irish ice sheets — is an interesting research topic worthy of further investigation.

## Conclusions

We find convincing evidence for surging, rapid retreat and stagnation of a former tidewater glacier draining the Younger Dryas Skye Icefield in NW Scotland. Not only does the well-preserved geomorphology indicate surging behaviour (i.e., oversized arcuate terminal moraines with mud aprons, small De Geer moraines, elongate fluted bedforms, ice-stagnation terrain), the glacier geometry (long, low-gradient glacier), substrate (soft deformable sediment) and setting (terrestrial-alpine to unconfined tidewater) match those most associated with surge-type glaciers in Arctic settings. Not all diagnostic surging landform features are present in this fjord, but they rarely are in palaeo systems. However, it is our opinion that the rarity of the landform assemblage — not yet seen in other Scottish fjords — indicates a distinct and unusual set of glaciological conditions signalling system change and/or dynamic instability.

We find evidence for three surges of the tidewater Ainort Glacier, each one slightly less extensive than the one before. The extent of the first and second surges corresponds well with the previously mapped limits of the YD Stadial glacier in this catchment. The final surge was followed by an uninterrupted quiescent phase that ultimately led to glacier demise. Submarine geomorphological evidence offers unique insight into glacier recession rates during the Younger Dryas Stadial in Scotland. Annual De Geer moraines indicate that post-surge grounding-line retreat up-fjord started slowly ( $\sim 50 \text{ ma}^{-1}$ ), perhaps in the presence of land-fast sea ice, accelerating to  $\sim 150 \text{ ma}^{-1}$  in mid-fjord and possibly  $\sim 300 \text{ ma}^{-1}$  at the fjord head. Our results show that the 3.5-km-long tidewater portion of the glacier may have disintegrated in as little as 20 years.

This work highlights the importance of identifying surge-type glaciers in palaeoglaciological studies, especially when exploring potential causes of asynchronous ice-mass response in the Quaternary record. Furthermore, this work serves as a test of Benn's hypothesis (2021) that surge-type glaciers existed on Skye, and probably elsewhere in Scotland, during the YD Stadial. We show not only that the landform assemblage in Loch Ainort is entirely 'consistent with repeated surges' (Benn, 2021: p. 16) but that this sea loch possesses the best geomorphological evidence of glacier surging so far identified in the British Isles. That being said, we end with a caveat:

identifying glacier surges in the palaeo record is not easy or clear cut. We accept that other glacier-dynamic interpretations are possible. However, in Loch Ainort, we argue that all the convergent lines of evidence point towards glacier surging — rapid advance, quiescence and then senescence — as the most likely mode of operation.

Finally, it is worth stressing the excellent state of preservation of the whole landform assemblage — something that is rare in Pleistocene systems in the British Isles. The seabed landforms in Loch Ainort could be said to be 'frozen in time', essentially unmodified and free from the deleterious effects of subaerial weathering, terrestrial erosion, periglacial processes and human disturbance over the intervening  $\sim 12,000$  years. Protection of these features for scientific posterity should be a priority.

**Acknowledgements.** The use of Maritime & Coastguard Agency MBES data (Crown Copyright), collected as part of the UKHO Civil Hydrography Programme, is gratefully acknowledged. Allan Audsley is thanked for his help resolving some GIS issues. We thank Brian Todd and an anonymous reviewer for their comments on this manuscript.

## Data Availability Statement

Bathymetry data access is available at: <https://datahub.admiralty.co.uk/portal/apps/sites/#/marine-data-portal>. All other derived data and calculations supporting the findings of the study are available from the lead author upon reasonable request.

## References

- Arosio, R., Gafeira, J., De Clippele, L.H., Wheeler, A.J., Huvenne, V.A., Sacchetti, F. et al. 2024. CoMMA: a GIS geomorphometry toolbox to map and measure confined landforms. *Geomorphology*, 458, 109227.
- Ballantyne, C.K. (1989) The Loch Lomond Readvance on the Isle of Skye, Scotland: glacier reconstruction and palaeoclimatic implications. *Journal of Quaternary Science*, 4, 95–108.
- Ballantyne, C.K. & Small, D. (2019) The last Scottish Ice Sheet. *Earth & Environmental Science Transactions, Royal Society of Edinburgh*, 110, 93–131.
- Ballantyne, C.K., Benn, D.I. & Small, D. (2016) The glacial history of Skye 2: The Loch Lomond Readvance. In: Ballantyne C.K. & Lowe J.J. (Eds.) *The Quaternary of Skye: Field Guide*, Quaternary Research Association: London; 23–40.
- Batchelor, C., Dowdeswell, J., Hogan, K., Larter, R., Parsons, E. & West, O. 2019. Processes and patterns of glacier-influenced sedimentation and recent tidewater glacier dynamics in Darbel Bay, western Antarctic Peninsula. *Antarctic Science*, 31: 218–227.
- Benn, D.I. (1991) Glacial sediments and landforms on Skye. In *The Quaternary of the Isle of Skye*, Quaternary Research Association: Cambridge; 35–67.
- Benn, D.I. (1992) The genesis and significance of 'hummocky moraine': evidence from the Isle of Skye, Scotland. *Quaternary Science Reviews*, 11, 781–799.
- Benn, D.I. (1997) Glacier fluctuations in Western Scotland. *Quaternary International*, 38/39, 137–147.
- Benn, D.I. (2021) Surging glaciers in Scotland. *Scottish Geographical Journal*, 137, 1–40.
- Benn, D.I. & Evans, D.J.A. (2014) *Glaciers and Glaciation*. Routledge: New York.
- Benn, D.I. & Lukas, S. (2006) Younger Dryas glacial landsystems in North-West Scotland: an assessment of modern analogues and palaeoclimatic implications. *Quaternary Science Reviews*, 25, 2390–2408.
- Benn, D.I., Fowler, A.C., Hewitt, I. & Sevestre, H. (2019) A general theory of glacier surges. *Journal of Glaciology*, 65, 701–716.
- Benn, D.I., Kirkbride, M.P., Owen, L.A. & Brazier, V. (2003) Glaciated Valley Landsystems. In *Glacial Landsystems*, Evans, D.J.A. (ed). Arnold: London; 372–406.

- Benn, D.I., Lowe, J.J. & Walker, M.J.C. (1992) Glacier response to climatic change during the Loch Lomond Stadial and early Flandrian: geomorphological and palynological evidence from the Isle of Skye, Scotland. *Journal of Quaternary Science*, 7, 125–144.
- Bennett, M.R. & Boulton, G.S. (1993) Deglaciation of the Younger Dryas or Loch Lomond Stadial ice-field in the northern Highlands, Scotland. *Journal of Quaternary Science*, 8, 133–145.
- Bickerdike, H.L., Evans, D.J.A., Ó Cofaigh, C. & Stokes, C.R. (2016) The glacial geomorphology of the Loch Lomond Stadial in Britain: a map and geographic information system resource of published evidence. *Journal of Maps*, 12, 1178–1186.
- Bickerdike, H.L., Evans, D.J.A., Stokes, C.R. & Ó Cofaigh, C. (2018) The glacial geomorphology of the Loch Lomond (Younger Dryas) Stadial in Britain: a review. *Journal of Quaternary Science*, 33, 1–54.
- Boston, C.M., Lukas, S. & Carr, S.J. (2015) A Younger Dryas plateau icefield in the Monadhliath, Scotland, and implications for regional palaeoclimate. *Quaternary Science Reviews*, 108, 139–162.
- Bradwell, T., Fabel, D., Clark, C.D., Chiverrell, R.C., Small, D., Smedley, R.K. et al. (2021) Pattern, style and timing of British–Irish Ice Sheet advance and retreat over the last 45 000 years: evidence from NW Scotland and the adjacent continental shelf. *Journal of Quaternary Science*, 36, 871–933.
- Brook, M., Hagg, W. & Winkler, S. (2013) Debris cover and surface melt at a temperate maritime alpine glacier: Franz Josef Glacier, New Zealand. *New Zealand Journal of Geology and Geophysics*, 56, 27–38.
- Burton, D.J., Dowdeswell, J.A., Hogan, K.A. & Noormets, R. (2016) Little Ice Age terminal and retreat moraines in Kollerfjorden, NW Spitsbergen. *Geological Society, London, Memoirs*, 46, 71–72.
- Capt, M., Bosson, J.B., Fischer, M., Micheletti, N. & Lambiel, C. (2016) Decadal evolution of a very small heavily debris-covered glacier in an Alpine permafrost environment. *Journal of Glaciology*, 62, 535–551.
- Chandler, B.M.P., Boston, C.M. & Lukas, S. (2019) A spatially restricted Younger Dryas plateau icefield in the Gaick, Scotland: reconstruction and palaeoclimatic implications. *Quaternary Science Reviews*, 211, 107–135.
- Chandler, B.M., Evans, D.J.A., Chandler, S.J., Ewertowski, M.W., Lovell, H., Roberts, D.H. et al. 2020. The glacial landsystem of Fjallsjökull, Iceland: spatial and temporal evolution of process-form regimes at an active temperate glacier. *Geomorphology*, 361, 107192.
- Clarke, G.K.C. (1991) Length, width and slope influences on glacier surging. *Journal of Glaciology*, 37, 236–246.
- Dix, J.K. & Duck, R.W. (2000) A high-resolution seismic stratigraphy from a Scottish sea loch and its implications for Loch Lomond Stadial deglaciation. *Journal of Quaternary Science*, 15, 645–656.
- Dowdeswell, J.A., Canals, M., Jakobsson, M., Todd, B.J., Dowdeswell, E.K. & Hogan, K.A. (2016) The variety and distribution of submarine glacial landforms and implications for ice-sheet reconstruction. *Geological Society London, Memoirs*, 46, 519–552.
- Ely, J.C., Clark, C.D., Spagnolo, M., Stokes, C.R., Greenwood, S.L., Hughes, A.L. et al. 2016. Do subglacial bedforms comprise a size and shape continuum? *Geomorphology*, 257, 108–119.
- Evans, D.J.A. & Wilson, S.B. (2006) Scottish landform example 39: The lake of Menteith glaciotectionic hill-hole pair. *Scottish Geographical Journal*, 122, 352–364.
- Finlayson, A., Golledge, N., Bradwell, T. & Fabel, D. (2011) Evolution of a Lateglacial mountain icecap in northern Scotland. *Boreas*, 40, 536–554.
- Flink, A.E., Noormets, R. & Kirchner, N. (2016) Annual moraine ridges in Tempelfjorden, Spitsbergen. *Geological Society London, Memoirs*, 46, 75–76.
- Flink, A.E., Noormets, R., Kirchner, N., Benn, D.I., Luckman, A. & Lovell, H. (2015) The evolution of a submarine landform record following recent and multiple surges of Tunabreen glacier, Svalbard. *Quaternary Science Reviews*, 108, 37–50.
- Golledge, N.R., Hubbard, A. & Sugden, D.E. (2008) High-resolution numerical simulation of Younger Dryas glaciation in Scotland. *Quaternary Science Reviews*, 27, 888–904.
- Golledge, N.R., Hubbard, A.L. & Sugden, D.E. (2009) Mass balance, flow and subglacial processes of a modelled Younger Dryas ice cap in Scotland. *Journal of Glaciology*, 55, 32–42.
- Grant, K.L., Stokes, C.R. & Evans, I.S. (2009) Identification and characteristics of surge-type glaciers on Novaya Zemlya, Russian Arctic. *Journal of Glaciology*, 55, 960–972.
- Gray, J.M. (1975) The Loch Lomond Readvance and contemporaneous sea-levels in Loch Etive and neighbouring areas of western Scotland. *Proceedings of the Geologists' Association*, 86, 227–238.
- How, P., Schild, K.M., Benn, D.I., Noormets, R., Kirchner, N., Luckman, A. et al. (2019) Calving controlled by melt undercutting: detailed calving styles revealed through time-lapse observations. *Annals of Glaciology*, 60, 20–31.
- Howe, J.A., Dove, D., Bradwell, T. & Gafeira, J. (2012) Submarine geomorphology and glacial history of the Sea of the Hebrides, UK. *Marine Geology*, 315–318, 64–76.
- Jasiewicz, J. & Stepinski, T.F. (2013) Geomorphons—a pattern recognition approach to classification and mapping of landforms. *Geomorphology*, 182, 147–156.
- Jiskoot, H., Murray, T. & Boyle, P. (2000) Controls on the distribution of surge-type glaciers in Svalbard. *Journal of Glaciology*, 46, 412–422.
- Kristensen, L., Benn, D.I., Holmes, A. & Ottesen, D. (2009) Mud aprons in front of Svalbard surge moraines: evidence of subglacial deforming layers or proglacial glaciotectionics? *Geomorphology*, 111, 206–221.
- Lovell, H., Benn, D.I., Lukas, S., Ottesen, D., Luckman, A., Hardiman, M. et al. (2018) Multiple Late Holocene surges of a High-Arctic tidewater glacier system in Svalbard. *Quaternary Science Reviews*, 201, 162–185.
- Lowe, J., Matthews, I., Mayfield, R., Lincoln, P., Palmer, A., Staff, R. et al. (2019) On the timing of retreat of the Loch Lomond ('Younger Dryas') Readvance icefield in the SW Scottish Highlands and its wider significance. *Quaternary Science Reviews*, 219, 171–186.
- Luckman, A., Benn, D.I., Cottier, F., Bevan, S., Nilsen, F. & Inall, M. (2015) Calving rates at tidewater glaciers vary strongly with ocean temperature. *Nature Communications*, 6, 8566.
- MacLeod, A., Palmer, A., Lowe, J., Rose, J., Bryant, C. & Merritt, J. (2011) Timing of glacier response to Younger Dryas climatic cooling in Scotland. *Global and Planetary Change*, 79, 264–274.
- Meier, M.F. & Post, A. (1969) What are glacier surges? *Canadian Journal of Earth Sciences*, 6, 807–817.
- Murray, T., Strozzi, T., Luckman, A., Jiskoot, H. & Christakos, P. (2003) Is there a single surge mechanism? Contrasts in dynamics between glacier surges in Svalbard and other regions. *Journal of Geophysical Research: Solid Earth*, 108, B5.
- Ottesen, D. & Dowdeswell, J.A. (2006) Assemblages of submarine landforms produced by tidewater glaciers in Svalbard. *Journal of Geophysical Research: Earth Surface*, 111, F1.
- Ottesen, D., Dowdeswell, J.A., Bellec, V.K. & Bjarnadóttir, L.R. (2017) The geomorphic imprint of glacier surges into open-marine waters: examples from eastern Svalbard. *Marine Geology*, 392, 1–29.
- Ottesen, D., Dowdeswell, J.A., Benn, D.I., Kristensen, L., Christiansen, H.H., Christensen, O. et al. (2008) Submarine landforms characteristic of glacier surges in two Spitsbergen fjords. *Quaternary Science Reviews*, 27, 1583–1599.
- Palmer, A.P., Matthews, I.P., Lowe, J.J., MacLeod, A. & Grant, R. (2020) A revised chronology for the growth and demise of Loch Lomond Readvance ('Younger Dryas') ice lobes in the Lochaber area, Scotland. *Quaternary Science Reviews*, 248, 106548.
- Plassen, L., Vorren, T.O. & Forwick, M. (2004) Integrated acoustic and coring investigation of glacial deposits in Spitsbergen fjords. *Polar Research*, 23, 89–110.
- Rivers, G.E., Storrar, R.D., Jones, A.H. & Ojala, A.E.K. (2023) 3D morphometry of De Geer Moraines and crevasse-squeeze ridges: differentiating between pushing and squeezing mechanisms from remotely sensed data. *Quaternary Science Reviews*, 321, 108383.
- Sevestre, H. & Benn, D.I. (2015) Climatic and geometric controls on the global distribution of surge-type glaciers: implications for a unifying model of surging. *Journal of Glaciology*, 61, 646–662.
- Sharp, M. (1988) Surging glaciers: behaviour and mechanisms. *Progress in Physical Geography: Earth and Environment*, 12, 349–370.
- Shennan, I., Bradley, S.L. & Edwards, R. (2018) Relative sea-level changes and crustal movements in Britain and Ireland since the Last Glacial Maximum. *Quaternary Science Reviews*, 188, 143–159.

- Sissons, J.B. (1979) The Loch Lomond Stadial in the British Isles. *Nature*, 280, 199–203.
- Small, D., Rinterknecht, V., Austin, W., Fabel, D., Miguens-Rodriguez, M. & Xu, S. (2012) In situ cosmogenic exposure ages from the Isle of Skye, northwest Scotland: implications for the timing of deglaciation and readvance from 15 to 11 ka. *Journal of Quaternary Science*, 27, 150–158.
- Smeaton, C., Yang, H. & Austin, W.E.N. (2021) Carbon burial in the mid-latitude fjords of Scotland. *Marine Geology*, 441, 106618.
- Stefaniak, A.M., Robson, B.A., Cook, S.J., Clutterbuck, B., Midgley, N.G. & Labadz, J.C. 2021. Mass balance and surface evolution of the debris-covered Miage Glacier, 1990–2018. *Geomorphology*, 373, 107474.
- Stoker, M.S., Bradwell, T., Howe, J.A., Wilkinson, I.P. & McIntyre, K. (2009) Lateglacial ice-cap dynamics in NW Scotland: evidence from the fjords of the Summer Isles region. *Quaternary Science Reviews*, 28, 3161–3184.
- Stokes, C.R. & Clark, C.D. (2002) Are long subglacial bedforms indicative of fast ice flow? *Boreas*, 31, 239–249.
- Thorp, P.W. (1991) Surface profiles and basal shear stresses of outlet glaciers from a Late-glacial mountain ice field in western Scotland. *Journal of Glaciology*, 37, 77–88.
- Truffer, M., Kääh, A., Harrison, W.D., Osipova, G.B., Nosenko, G.A., Espizua, L. et al. (2021) Glacier surges. In *Snow and Ice-related Hazards, Risks, and Disasters*. Elsevier: Amsterdam; 417–466.